communications medicine

A Nature Portfolio journal

Article

https://doi.org/10.1038/s43856-026-01629-z

Circulating EV-microRNAs are dynamic biomarkers of resistance to therapeutic immunomodulation in metastatic melanoma

Elena Splendiani[1,12], Zein Mersini Besharat[1,2,12], Claudia Sabato[3,12], Teresa Maria Rosaria Noviello[2], Maria Fortunata Lofiego[4,5], Vincenzo D'Alonzo[4], Monica Valente[4], Laura Solmonese[5], Alessia Covre[5], Sandra Coral[5], Francesca Pia Caruso[6,7], Tanja Milena Autilio[1], Ines Simeone[8], Agnese Po[9], Anna Citarella[10], Giuseppina Catanzaro[10], Roberta Mortarini[11], Andrea Anichini[11], Michele Maio[4,5], Michele Ceccarelli[2], Anna Maria Di Giacomo[4,5] ✉ & Elisabetta Ferretti[1] ✉

Abstract

Background Melanoma is the most aggressive skin cancer, with a 50% five-year mortality in metastatic or unresectable cases. Non-invasive biomarkers are crucial for guiding treatment. MicroRNAs (miRNAs), especially those encapsulated in extracellular vesicles (EVs), are stable in plasma and hold promise as biomarkers.

Methods This study analyzed EV-associated miRNAs (EV-miRNAs) from 50 blood samples of 18 stage III-IV melanoma patients treated with anti-CTLA-4 immunotherapy and a DNA hypomethylating agent. Samples were collected at baseline, week 4, and week 12. Patients were classified as responders (R) or non-responders (NR).

Results A baseline signature of four EV-miRNAs predicted primary resistance. Treatment altered 15 EV-miRNAs at week 4 and 51 at week 12; nine were consistently modulated. At week 12, 27 EV-miRNAs differed between NR and R, with miR-1203 and miR-566-3p up-regulated in NR, linked to resistance and poor survival.

Conclusions These results highlight EV-miRNAs as non-invasive biomarkers for predicting and monitoring therapy response.

Plain language summary

This study aimed to develop easy and minimally invasive methods to predict and monitor how patients with advanced melanoma respond to immunotherapy and epigenetic treatments. Melanoma is a serious and often deadly skin cancer, and better tools are needed to guide treatment decisions. The researchers studied microRNAs, small molecules found in particles in the blood, from melanoma patients before and during treatment. They found specific microRNAs that can predict which patients may not respond to therapy. These blood-based microRNA biomarkers could help physicians to personalize the treatments, leading to more effective care and better outcomes for patients in the future.

In recent years, microRNAs (miRNAs) have gained prominence as biomarkers for monitoring therapeutic responses in cancer due to their regulatory roles in cellular processes and their ability to reflect disease states, particularly in complex malignancies, such as advanced melanoma[1–3].

In fact, despite the progress achieved in advanced melanoma treatment with innovative therapies, such as immunotherapy, challenges remain since a significant subset of patients either fail to respond or eventually develop resistance to these therapies[4–6].

[1]Department of Experimental Medicine, Sapienza University, Rome, Italy. [2]Sylvester Comprehensive Cancer Center, Department of Public Health Sciences, Miller School of Medicine, University of Miami, Miami, FL, USA. [3]Laboratory of Preclinical and Translational Research, IRCCS CROB Centro di Riferimento Oncologico della Basilicata, Rionero in Vulture, Italy. [4]Center for Immuno-Oncology, Medical Oncology and Immunotherapy, Department of Oncology, University Hospital of Siena, Siena, Italy. [5]Medical Oncology, Department of Molecular and Developmental Medicine, University of Siena, Siena, Italy. [6]Istituto di Ricerche Genetiche "Gaetano Salvatore", Biogem Scarl, Ariano Irpino, Italy. [7]Department of Electrical Engineering and Information Technology, University of Naples Federico II, Naples, Italy. [8]Humanitas Research, Rozzano, Italy. [9]Department of Radiological, Oncological & Pathological Sciences, Sapienza University, Rome, Italy. [10]Department of Life Sciences, Health and Health Professions, Link Campus University, Rome, Italy. [11]Human Tumor Immunobiology Unit, Department of Research, Fondazione IRCCS Istituto Nazionale dei Tumori, ENETS Center of Excellence, Milan, Italy. [12]These authors contributed equally: Elena Splendiani, Zein Mersini Besharat, Claudia Sabato. ✉e-mail: annamaria.digiacomo@unisi.it; elisabetta.ferretti@uniroma1.it

Identifying reliable biomarkers to predict and monitor therapeutic responses is critical for enhancing clinical management and personalizing treatment strategies for these patients.

In this study, we employed liquid biopsy as a noninvasive sampling method to identify precise EV-miRNAs as biomarkers of therapeutic response in advanced melanoma (stage III–IV), and specifically, we analyzed miRNAs encapsulated in extracellular vesicles (EV-miRNAs)[1,7–9].

Our analysis focused on a cohort of advanced melanoma patients enrolled in the phase Ib NIBIT-M4 study (NCT02608437), who received a combination therapy of the monoclonal antibody anti-CTLA-4 (ipilimumab) and the DNA hypomethylating agent (DHA), guadecitabine.

We analyzed plasma samples collected both before and during treatment to assess EV-miRNAs modulated throughout therapy. This approach enabled the identification of EV-miRNAs associated with both primary and acquired therapeutic resistance.

Overall, our findings demonstrate that circulating EV-miRNAs serve as biomarkers to predict and monitor therapeutic immunomodulation response in advanced melanoma.

Methods

Ethics approval

Ethical approval for the parent clinical trial and for the present translational study was obtained from the University Hospital of Siena (Siena, Italy) and Sapienza University of Rome. The phase Ib NIBIT-M4 trial of guadecitabine plus ipilimumab in unresectable/metastatic melanoma was conducted under the authorization of the University Hospital of Siena (European Union Drug Regulating Authorities Clinical Trials number 2012-004301-27; ClinicalTrials.gov Identifier NCT02608437 registration date: 2015-11-13), and the results of the trial have been published in refs. 10,11. The evaluation of the circulating microRNA study reported here was further approved by the Ethics Committee of Sapienza University of Rome (Ethics Committee number 5943). All studies were conducted in accordance with the Declaration of Helsinki 1964 and its later amendments. All participating patients and subjects provided signed informed consent before enrollment.

Discovery cohort

We collected all available plasma samples from patients enrolled in the phase I NIBIT-M4 study conducted at the Center for Immuno-Oncology in Siena, ClinicalTrials.gov Identifier: NCT02608437[10]. The cohort consisted of 18 patients with unresectable metastatic melanoma (stages III–IV), and samples were collected at three time points. Patients received DHA (guadecitabine) at escalating doses following a 3 + 3 dose-escalation design, with doses of 30, 45, or 60 mg/m² administered on days 1–5 during weeks, week 0 (W0), W3, W6, and W9. Immunotherapy (Ipilimumab) was administered at 3 mg/kg during weeks W4, W7, and W10. Tumor responses to immunotherapy were evaluated at baseline (W0) and subsequently at W12.

Plasma samples were collected at baseline (W0) and at W4 and W12, resulting in a total of 50 plasma samples. It should be noted that four patients did not reach the W12 timepoint. This cohort served as the discovery cohort for our study (Table 1).

Table 1 | Discovery cohort

Patient ID	Week 0 *n* = 18	Week 4 *n* = 18	Week 12 *n* = 14	BOR	Gender	BRAF status	M stage
MM_001	X	X	X	PD	F	MUT	M1c
MM_002	X	X	X	PD	M	MUT	M1a
MM_003	X	X	X	CR	M	NA	M1a
MM_004	X	X	X	PR	M	WT	M1a
MM_005	X	X	–	CR	M	WT	IIIC
MM_006	X	X	–	PD	M	MUT	M1a
MM_007	X	X	X	PD	M	WT	IIIC
MM_008	X	X	X	PD	M	MUT	M1c
MM_011	X	X	X	SD	M	WT	M1a
MM_012	X	X	X	SD	F	WT	M1a
MM_013	X	X	X	PD	F	WT	M1a
MM_014	X	X	X	PR	M	WT	M1c
MM_015	X	X	X	PD	M	WT	M1c
MM_016	X	X	X	PD	M	WT	M1b
MM_017	X	X	X	SD	M	WT	M1c
MM_018	X	X	X	PR	M	MUT	M1a
MM_020	X	X	–	PD	M	WT	M1a
MM_021	X	X	–	PD	M	WT	M1a

Overview of clinical characteristics of the NIBIT-M4 cohort screened for EV-miRNAs expression. It includes the number of participants evaluated at each time point, categorized by best overall response (BOR) as progression disease (PD), stable disease (SD), partial response (PR), and complete response (CR), according to irRC criteria. Additionally, the table presents data on gender (female and male), BRAF V600 mutation status: BRAF mutated (MUT) and BRAF wild type (WT), and disease stage (M stage).

Table 2 | Validation cohort

Gender	
Male	4 (50.0%)
Female	4 (50.0%)
BOR	
PR	2 (25%)
SD	1 (12.5%)
CR	1 (12.5%)
PD	4 (50.0 %)

Overview of clinical characteristics of the validation cohort screened for seven EV-miRNAs biomarkers of primary resistance. Best overall response (BOR), progression disease (PD), partial response (PR), and complete response (CR).

Validation cohort

To validate the EV-miRNAs identified as primary resistance biomarkers for the combination therapy, an independent cohort of 8 metastatic melanoma patients treated with ipilimumab monotherapy (4 R and 4 NR) was used. Serum samples were collected from these patients before therapy, and EVs were isolated using the same extraction protocol employed for the main cohort. The levels of 7 predictive EV-miRNAs were quantified using droplet digital PCR (ddPCR). Details of the validation cohort are provided in Table 2.

EV isolation and RNA extraction

Blood samples were collected in EDTA tubes and processed within 30 min to isolate plasma. The EVs were isolated using the polymer precipitation method (Cat# EQULTRA-20A-1 System Biosciences SBI, Palo Alto, CA) plus thrombin pre-clearing Cat# TMEXO-1, System Biosciences SBI, Palo Alto, CA) as previously described[12].

Transmission electron microscopy (TEM) of EVs was performed as previously described[12]. Briefly, EVs were fixed in 4% paraformaldehyde and adsorbed on formvar-carbon-coated copper grids. The grids were then incubated in 1% glutaraldehyde for 5 min, washed with deionized water eight times, and then negatively stained with 2% uranyl oxalate (pH 7) for 5 min and methyl cellulose/uranyl for 10 min at 4 °C. Excess methyl cellulose/uranyl was blotted off, and the grids were air-dried and observed in TEM (Morgagni 268D, Philips Electronics, Eindhoven, The Netherlands) at an accelerating voltage of 80 kV. Digital images were taken with Mega View imaging software.

The particle size distribution and concentration of purified EVs from plasma samples of melanoma patients were determined by exoid tunable resistive pulse sensing measurement system (Izon Science, USA) and

analyzed with Izon Control Suite Software (version 1.0.2.32). To determine the particle concentration, for each sample, an average of 500 particles were counted and compared with the size and concentration reference calibration particles (Izon Science, USA). A 150 nm polyurethane nanopore membrane (Izon Science, USA) was stretched at 47 mm by applying the pressure at 300 Pa and voltage at 700 mV. Western blot analysis of EVs was performed, reporting positive staining for the canonical vesicle markers (HSP70, TSG101, CD63 and CD81) and absence of the intracellular marker calnexin, as described in ref. 12.

For RNA isolation, the EVs were processed using the Maxwell RSC miRNA Plasma and Serum Kit (Cat# AS1680, Promega). To evaluate RNA extraction efficiency, a synthetic spike-in (Ath-miR-159a) was added to the samples post-lysis to achieve a final concentration of 4 pM.

Extraction efficiency was assessed by real-time PCR (RT-qPCR) for the spike-in control, using a mean Ct value of 23 as the threshold for successful extraction.

EV-miRNAs Profiling Analysis

Samples were profiled using the RT-qPCR panel of 754 miRNAs on TaqMan Advanced miRNA Human A and B Cards (Cat# A31805; ThermoFisher Scientific, Rockford, USA). Data were preprocessed by cleaning, filtering, and normalizing the expression levels (HTqPCR package, Bioconductor http://www.r-project.org/).

Cycle thresholds (Ct) classified as "undetermined" were assigned to the value of Ct = 40, and EV-miRNAs with Ct values > 33 were considered not expressed and were excluded from further analysis. Only EV-miRNAs with Ct values ≤ 33 were deemed informative (as per manufacturer's recommendation[13]) and included in subsequent expression analysis. The norm.Rank invariant method was applied for normalization. DE analysis of EV-miRNAs was conducted using normalized data, calculating the delta-delta Ct (ddCT) method and expressing the fold change as $2^{(-\mathrm{ddCT})}$. EV-miRNAs with a fold change >|2| and a $p < 0.05$ were considered DE. The p-value was calculated using the Wilcoxon–Mann–Whitney test.

EV-miRNAs signature in internal validation cohort by droplet digital PCR

Seven EV-miRNAs were analyzed in an independent internal validation cohort, as described above (Table 2). EV-miRNAs levels were quantified using ddPCR (Bio-Rad Laboratories, Hercules, CA). A universal reverse transcription was performed for each sample starting from 2 µl of RNA using TaqMan™ Advanced miRNA cDNA Synthesis Kit (Cat# A28007, Applied Biosystem) with miR-Amp reaction step, following manufacturer instructions. Then ddPCR was performed following the manufacturer instruction. MiRNA assays ID: 479018_mir hsa-miR-548b-3p; ID: 479075_mir hsa-miR-592-5p; ID: 478486_mir hsa-miR-199b-5p; ID: 479224_mir hsa-miR-99a-3p; ID: 477942_mir hsa-miR-188-3p; ID: 477910_mir hsa-miR-142-3p; ID: 478138_mir hsa-miR-497-5p; ThermoFisher Scientific).

Statistical analysis

Statistical analyses on DE EV-miRNAs were conducted using R or Python programming environment. The Wilcoxon Mann–Whitney test was applied, and results were considered statistically significant when p-values were <0.05. For additional statistical tests, including the ddPCR, GraphPad Prism software (Version 8.3, La Jolla, California, USA) was used. In detail, the Wilcoxon Mann–Whitney test was also employed to compare EV-miRNAs levels between experimental groups, with statistical significance defined as $p < 0.05$. The receiver operating characteristic (ROC) analyses for the discovery and validation cohorts were performed using different combinations of the 7 EV-miRNAs signature of primary resistance. The combination of microRNAs that provided the best performance in terms of AUC in both cohorts was selected.

Count per million expression profiles of the 7 EV-miRNAs signature of primary resistance were retrieved from the FANTOM5 database for cell type enrichment.

Both KEGG and GO (biological process) data from miRPath v.4 were used in the target enrichment analysis[14]. The following parameters were used: validated miRNA target genes selected from Tarbase v8.0, selected miRNA annotation from miRbase v22.1, gene union as merging method, Classical analysis, FDR correlation, p-value threshold 0.05.

For miR-1203 and miR-556-3p multivariate COX proportional hazard model analysis, ROC and Kaplan–Meier analyses were performed in R using packages survivalROC, survminer, survival and ggplot2. Visualization of data was performed in Python environment using the Seaborn and Matplotlib packages.

Results

EV-miRNAs profiling

Considering the growing need for effective and minimally invasive biomarkers to monitor therapy response, we collected and analyzed 50 blood samples from 18 patients with advanced melanoma (stages III and IV), who participated in the phase Ib NIBIT-M4 clinical trial and were broadly characterized for different molecular aspects[10,11]. Samples were collected at three time points: baseline (week 0), week 4, and week 12 (end of treatment). The study workflow is summarized in Fig. 1.

At the end of treatment, clinicians evaluated patients and assessed the therapy response using computed tomography (CT) scans based on the immune-related response criteria (irRC): progression of disease (PD), stable disease (SD), partial response (PR), and complete response (CR). Eight patients (44.5%)—SD, PR, CR—were classified as responders (R), while 10 patients PD (55.5%) were classified as nonresponders (NR). Patients' features details are reported in Table 1.

EVs were isolated and characterized as described in Sabato et al.[12], resulting in multiple vesicles with a round-shaped morphology, a diameter of 100–400 nm and positive staining for vesicle markers (data not shown).

During RNA extraction, we introduced an exogenous miRNA as spike-in control: Ath-miR-159a and quantified its expression level to determine successful extractions. Two samples with Ct values exceeding 23 were excluded from further analysis (Supplementary Fig. 1a).

We then evaluated levels of EV-miRNAs expressions in the remaining 48 samples, and 526 EV-miRNAs were found to be consistently expressed (Supplementary Data 1).

EV-miRNAs profiling before therapy

We first investigated EV-miRNAs profiles of patients before therapy (week 0) and conducted a supervised analysis, comparing profiles from NR and R patients.

We were able to identify in NR patients 7 EV-miRNAs differentially expressed (DE) at the baseline, 3 up-regulated (miR-142-3p, miR-497-5p, and miR-188-3p) and 4 down-regulated (miR-548-3p, miR-99a-3p, miR-199-5p, and miR-592) (Fig. 2a and Supplementary Data 2).

To further explore the cellular origin of these EV-miRNAs, we queried the FANTOM5 database and examined the distribution of these EV-miRNAs across different cell types. As it is shown in Fig. 2b, the hierarchical clustering of immune and stromal cell populations revealed two primary clusters enriched with these EV-miRNAs. The first cluster predominantly consisted of immune cells, including NK cells, T cells, monocytes, and neutrophils, with miR-142-3p, miR-548b-3p, and miR-188-3p particularly enriched.

The second cluster was more heterogeneous and divided into two subgroups: one includes microenvironmental cells such as melanocytes, keratinocytes, endothelial cells, adipocytes, mesenchymal cells, and fibroblasts, with miR-497-5p and miR-99a highly expressed in endothelial cells and adipocytes, while miR-199b-5p was enriched in mesenchymal cells and fibroblasts.

A subgroup of the second cluster consisted of stem cells, with high expression of miR-592. These results allowed us to identify a set of EV-miRNAs that are specific of NR patients and can derive from different cell types, including immune cells.

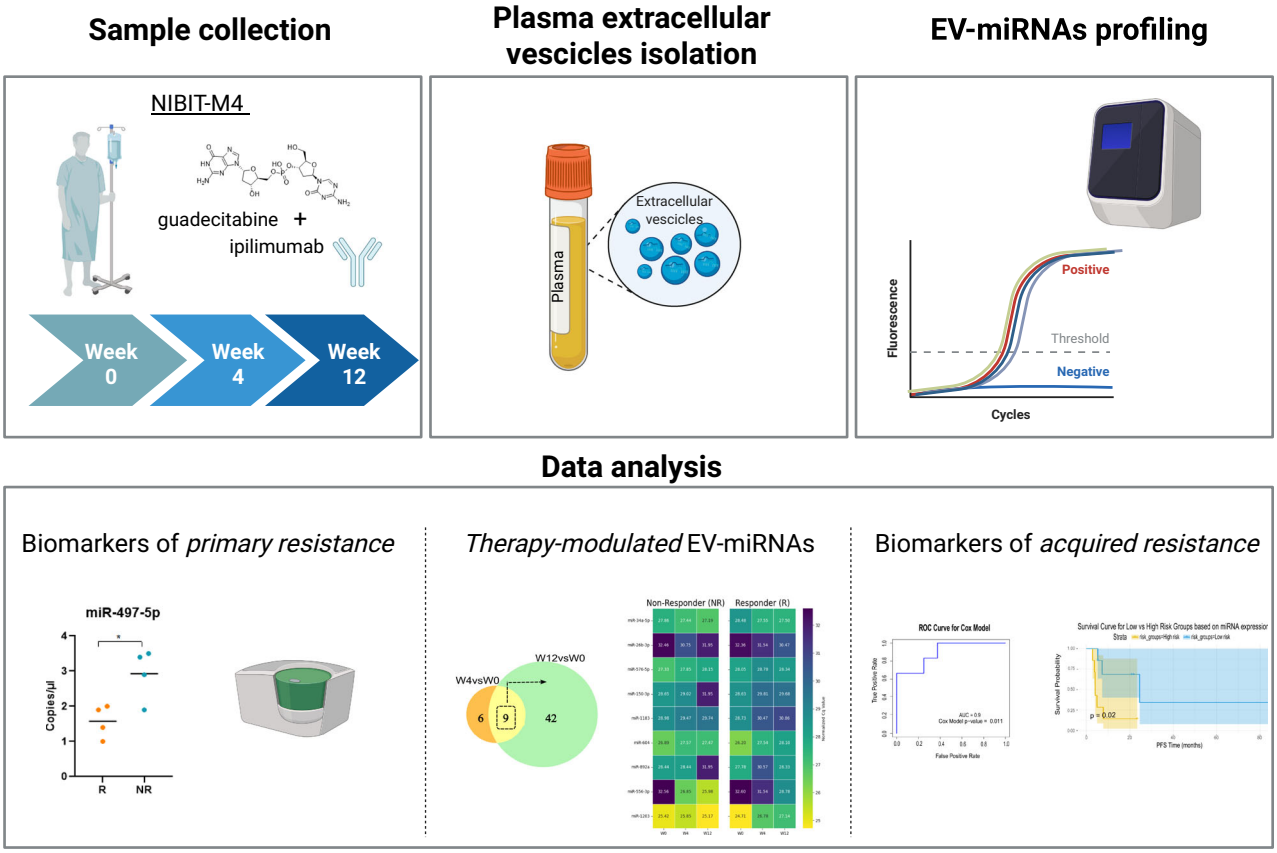

Fig. 1 | Workflow of the phase 1b NIBIT-M4 clinical study and EV-miRNAs profile. Blood samples were collected from patients with advanced melanoma (stages III and IV) at three time points: week 0, week 4, and week 12. EVs were isolated from plasma, and associated miRNAs were analyzed.

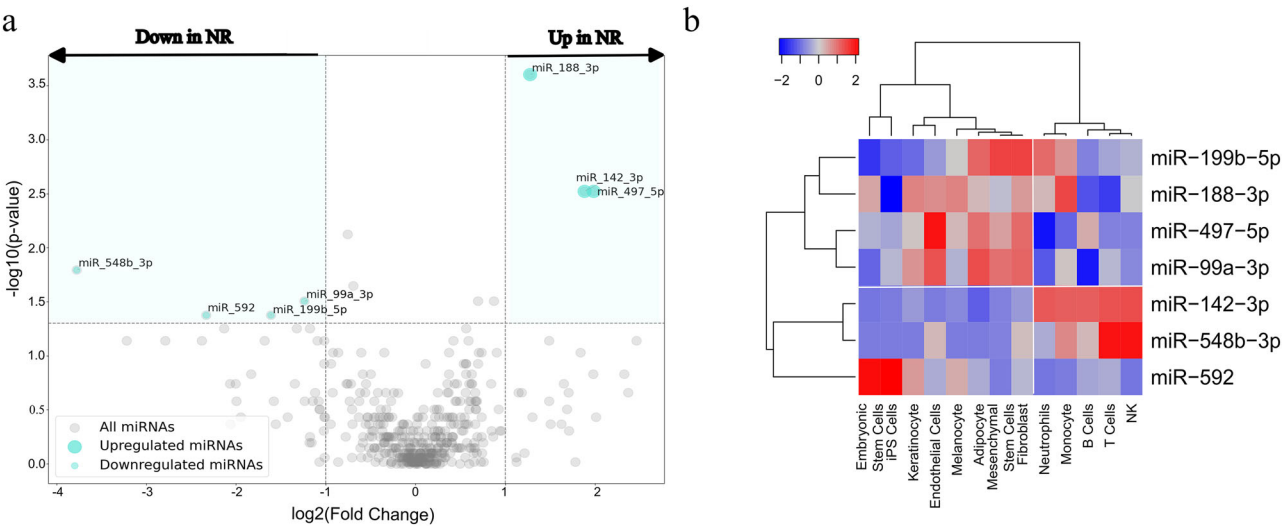

Fig. 2 | EV-miRNAs signature to predict primary resistance. a Volcano plot illustrates 7 EV-miRNAs DE between NR and R patients prior to treatment. The x-axis shows the $\log_2$ fold change, while the y-axis represents the -log10(*p*-value). Grey dots correspond to all EV-miRNAs analyzed, while highlighted light blue dots represent the statistically significant DE EV-miRNAs ($p < 0.05$ and fold change >|2|). **b** Heatmap showing average miRNAs expression across cell types from the FANTOM5 project. Each row represents a miRNA, and columns denote cell types with hierarchical relationships between cells (columns) and miRNAs (rows). Color intensity reflects miRNA expression ($\log_2$ Z-score).

EV-miRNAs biomarker of primary resistance: miR-497-5p, miR-99a-3p, miR-592, and miR-548b-3p

We confirmed the 7 EV-miRNAs biomarkers of primary resistance, originally identified in the discovery cohort, in a validation cohort of 8 patients treated with ipilimumab monotherapy. This new cohort consists of four R and four NR patients, for whom only serum samples were available (Table 2).

Using ddPCR, we evaluated whether the baseline expression levels of these EV-miRNAs could differentiate between patients classified as R or NR patients at the end of treatment according to irRC.

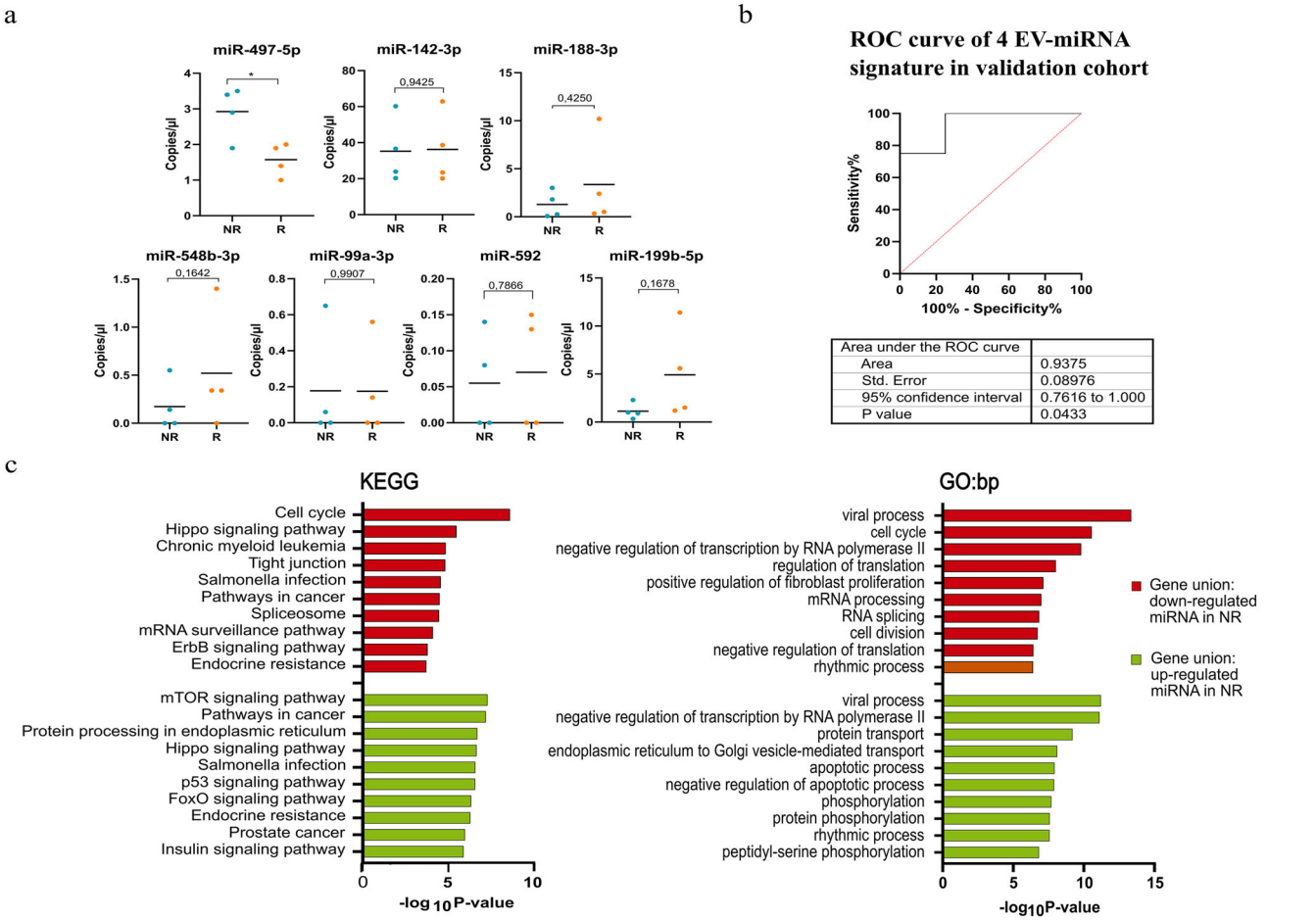

Fig. 3 | Validation of EV-miRNAs signature to predict resistance to immunotherapy. a Absolute quantification of the 7 EV-miRNAs signature of primary resistance in an independent cohort of metastatic melanoma patients treated with anti-CTLA4 only, using ddPCR. MiRNAs up-regulated (upper panel) and down-regulated (lower panel) in NR versus R. Statistical significance was determined using an unpaired t-test. **b** ROC Curve analysis of primary resistance EV-miRNAs signature (MiR-497-5p, miR-99a-3p, miR-592-5p, and miR-548b-3p) in the validation cohort. **c** Barplot of top 10 significantly enriched pathways for the 4 EV-miRNAs signature, computed as gene union for up-regulated (green) and down-regulated (red) EV-miRNAs in NR vs. R. $p < 0.05$ (*) were considered statistically significant. NR nonresponder, R responder, ROC receiver operating characteristic, ddPCR droplet digital PCR, bp biological process.

Among all, miR-497-5p showed significantly higher levels in NR compared to R (Fig. 3a and Supplementary Data 3).

Although the expression patterns of all down-regulated EV-miRNAs were consistent with the findings from the NIBIT-M4 cohort, none of them reached statistical significance individually.

To further assess the predictive value of the identified EV-miRNAs signature, we performed ROC curve analysis on both discovery and validation cohorts.

The best value of area under the curve (AUC) was reached combining miR-497-5p with miR-99a-3p, miR-592, and miR-548b-3p, indicating a predictive performance of AUC = 0.8 in the discovery (Supplementary Fig. 1b) and AUC = 0.94 (Fig. 3b) in the validation cohort.

To investigate the biological functions of the validated EV-miRNA signature in melanoma, pathway enrichment analysis using the validated target genes of the selected miRNA was performed, revealing significant associations with key tumorigenic pathways. EV-miRNAs down-regulated in NR were strongly linked to pathways promoting tumor growth, such as cell cycle regulation and Hippo signaling, suggesting a potential loss or attenuation of their tumor-suppressive role in these patients. Conversely, EV-miRNAs up-regulated in NR were associated with apoptotic and metabolic regulation pathways, including mTOR and p53, indicating activation of adaptive mechanisms that may contribute to tumor resistance. These findings highlight a dual functional role of EV-miRNAs in melanoma, where differential modulation reflects both tumor progression and cellular survival processes, providing critical insights for targeted therapeutic strategies (Fig. 3c and Supplementary Data 4).

Collectively, the results proposed the EV-miRNAs signature as a valuable predictor of ipilimumab resistance in patients with advanced melanoma.

Therapy-modulated EV-miRNA signature

To evaluate whether EV-miRNAs expression levels were modulated during treatment, we performed DE analysis at on-treatment time points relative to baseline (week 0). At week 4, 15 EV-miRNAs were DE, with 7 down-regulated and 8 up-regulated (Fig. 4a and Supplementary Data 5).

By week 12, the number increased significantly to 51, including 29 down-regulated and 22 up-regulated EV-miRNAs (Fig. 4b and Supplementary Data 5).

We next assessed those EV-miRNAs that were modulated in the two post-treatment time points. Notably, nine EV-miRNAs (miR-150-3p, miR-576-5p, miR-26b-3p, miR-34a-5p, miR-556-3p, miR-1183, miR-1203, miR-604, and miR-892a) were consistently dysregulated at both week 4 and week 12 (Fig. 4c and Supplementary Fig. 1c).

The validated target gene enrichment analysis of the nine EV-miRNAs reveals their involvement in key melanoma-associated signaling pathways, including MAPK, PI3K-AKT, p53 pathways, and cell cycle regulation, which are central to tumor growth and survival. Importantly, the targets of the up-regulated EV-miRNAs are significantly enriched in pathways related

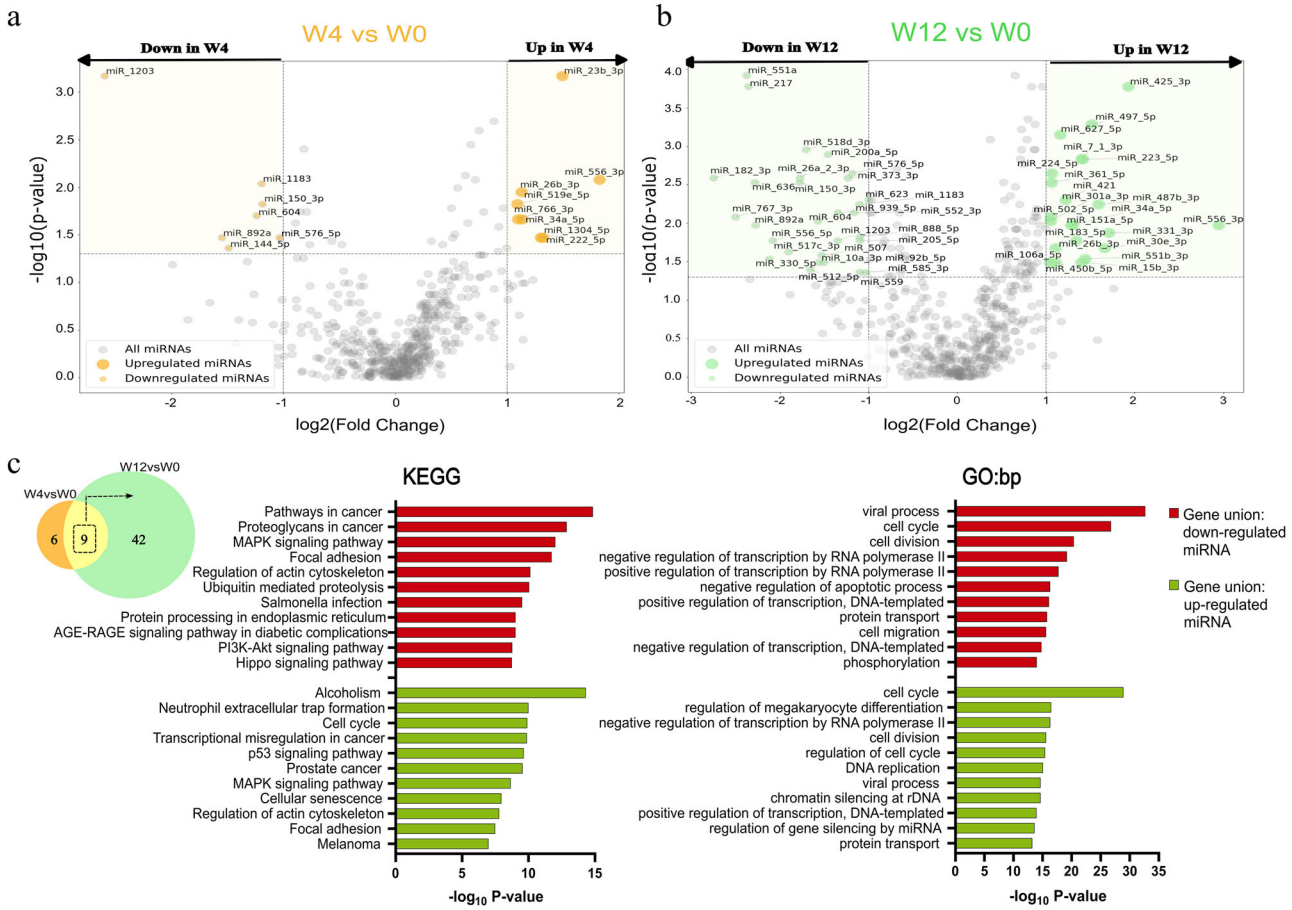

Fig. 4 | Dynamic regulation of EV-miRNAs during combined therapy. a Volcano plot illustrates the 15 EV-miRNAs DE between W4 and W0 in response to DHA plus ICB treatment. Each point represents EV-miRNAs, the x-axis shows the $\log_2$ fold change expression between W4 and W0, and the y-axis indicates the negative logarithm (base 10) of the *p*-value. Significant EV-miRNAs meeting the criteria of a fold change >|2| and a $p < 0.05$ are highlighted. **b** Similar to (**a**) but for the 51 EV-miRNAs DE between W12 and W0. **c** Top 11 significantly enriched pathways for the 9 EV-miRNAs commonly dysregulated after therapy (venn diagram), computed as gene union for up-regulated (green) and down-regulated (red) EV-miRNAs in W4 and W12 vs. W0. W0 week 0, W4 week 4, W12 week 12, DE differentially expressed, DHA DNA hypomethylating agent. ICB immune-checkpoint blockage, bp biological process.

not only to melanoma progression but also to hematopoietic processes, such as megakaryocyte differentiation and immune responses, including neutrophil extracellular trap formation (Fig. 4c and Supplementary Data 6). These findings underscore a complex and multifaceted role of EV-miRNAs in orchestrating melanoma pathogenesis, impacting both intrinsic tumor cell programs and the modulation of the tumor microenvironment.

Of note, among the EV-miRNAs significantly down-regulated at week 12, we identified two previously reported melanoma-specific diagnostic EV-miRNAs, miR-1203 and miR-507[12].

These findings suggest that dynamic on-treatment changes in EV-miRNAs reflect the effects of therapy and offer valuable insights into the underlying treatment mechanisms.

EV-miRNAs are biomarkers of acquired resistance associated with reduced progression-free and overall survival

To evaluate the potential association of EV-miRNAs with therapeutic outcomes, we performed a supervised DE analyses of EV-miRNA profiles between NR and R at week 12. As illustrated in the volcano plot (Fig. 5a), this analysis led to the identification of 27 EV-miRNAs, of which 7 were down-regulated and 20 up-regulated in NR compared to R (Supplementary Data 2). Among these, only two EV-miRNAs (miR-1203 and miR-556-3p) showed modulation at week 4 and week 12, one of which is miR-1203, a diagnostic biomarker of melanoma[12] (Fig. 5b).

These findings suggest that the identified EV-miRNAs may serve as potential biomarkers of acquired resistance. Their early modulation, observed as soon as 4 weeks post-treatment, highlights their utility for prognostic assessments and follow-up evaluations.

To explore the potential role of miR-1203 and miR-556-3p as biomarkers for predicting treatment failure, we analyzed their expression dynamics over time in the NIBIT-M4 trial cohort.

As shown in Fig. 6a and Supplementary Fig. 2a, b, expression trends for these EV-miRNAs were concordant across most patients, with clearer patterns emerging upon analysis of average expression levels. To evaluate their predictive potential, we applied a multivariate Cox proportional hazards model based on progression-free survival (PFS) and the expression levels of miR-1203 and miR-556-3p at week 12. The resulting ROC curve exhibits an AUC = 0.87 and a *p*-value of 0.001 (Fig. 6b). Using this model, we performed Kaplan–Meier survival analysis by stratifying patients into risk groups defined by the expression levels of the two EV-miRNAs. This analysis revealed that higher expression of both miR-1203 and miR-556-3p was significantly associated with shorter PFS over an 80-month follow-up period (Fig. 6c). A similar approach was applied to overall survival (OS) data. The resulting ROC curve yielded an AUC of 0.82 and a *p*-value of 0.043 (Fig. 6d). Kaplan–Meier analysis using the same EV-miRNA-defined risk groups confirmed that elevated expression of both EV-miRNAs was significantly associated with reduced OS (Fig. 6e and Supplementary Data 7). Notably, both models closely mirrored the Kaplan–Meier curves obtained using OS data (Supplementary Fig. 2c) and PFS data (Supplementary Fig. 2d) when stratified by treatment response status (responder or nonresponder).

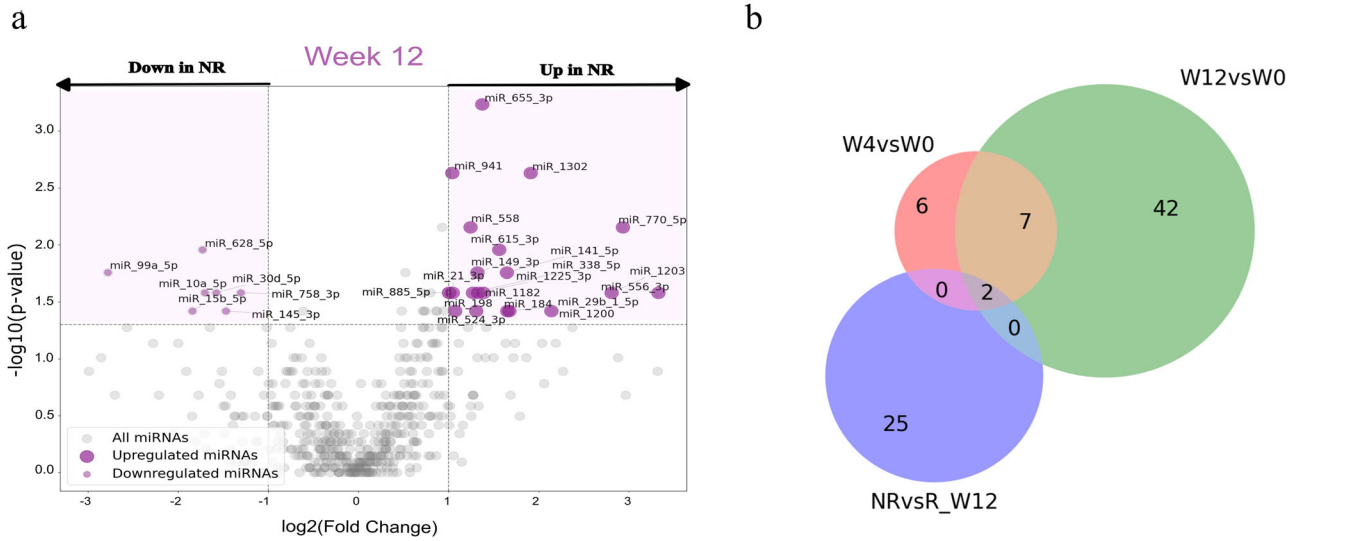

Fig. 5 | EV-miRNAs as biomarkers of acquired resistance in advanced melanoma. **a** Volcano plot illustrating 27 EV-miRNAs DE between NR and R at W12. The plot displays the $\log_2$ fold change on the x-axis and the -log10(*p*-value) on the y-axis. Grey dots represent all analyzed EV-miRNAs, while purple dots highlight statistically significant EV-miRNAs ($p < 0.05$ and fold change >|2|). **b** The Venn diagram shows the overlap of significant EV-miRNAs between the comparisons: W4 vs. W0, W12 vs. W0, and NR vs. R at W12. Numbers indicate the count of unique and overlapping significant EV-miRNAs among the groups. W0 week 0, W4 week 4, W12 week 12, R responder, NR nonresponder.

These findings underscore the prognostic value of miR-1203 and miR-556-3p in predicting therapeutic outcomes in metastatic melanoma treated with combined therapy of immune checkpoint blockage, with potential for early relapse monitoring at 4 weeks post-treatment.

Discussion

Liquid biopsy presents distinct advantages for late-stage patients by circumventing the need for traditional, often invasive tissue biopsies, which can be particularly burdensome and sometimes unfeasible in advanced stages[8,15].

In this context, miRNAs provide a comprehensive view of pathological states and can highlight disease-specific alterations, since they serve as fine regulators of cellular state. Their expression may reveal changes in cellular differentiation and regulatory pathways, making them highly specific and informative biomarkers in advanced melanoma[12,16].

Of note, EVs selectively package miRNAs that mirror the state of their cells of origin and protect them from circulating nucleases, thereby increasing their half-life and assay reproducibility in blood, thus showing better biomarker potential and diagnostic performance when compared to circulating free miRNA[17].

We therefore performed EV-miRNA profiling in order to (i) capture vesicle-enriched, disease-related miRNA signals that might be diluted in whole plasma, and (ii) exploit the greater biochemical stability conferred by vesicle encapsulation, which can improve robustness and clinical translatability of circulating miRNA biomarkers.

This study underscores the potential of EV-miRNAs as biomarkers for predicting both primary and acquired responses to therapies involving immune checkpoint inhibitors (ICI) and DHA. DHAs have been shown to enhance the efficacy of various immunotherapeutic agents, making them promising adjuncts in combination therapy approaches[10,11,18,19].

The NIBIT-M4 clinical trial enabled us to evaluate EV-miRNAs and identify biomarkers of primary and acquired resistance in a well characterized cohort of patients[10–12], addressing a disease where lack of biomarkers remains a challenge. The strength of this study, as well as its primary limitation, lies in the uniqueness of this patient cohort. Given that this was an exploratory clinical trial investigating a novel combination therapy, guadecitabine plus ipilimumab, no independent cohorts with the same treatment are currently available. This limited the ability to validate the identified EV-miRNAs post-therapy in an external cohort. Nevertheless, we investigated whether the identified signature might be applicable to patients undergoing ipilimumab monotherapy.

We identify a signature of EV-miRNAs capable of distinguishing, at baseline, patients who are likely to exhibit therapy resistance (Table 3). Of note, evaluation of the immunophenotype of the NR and R patients did not provide evidence regarding the EV-miRNAs origin, and in vitro experiments in primary melanoma cells lines treated with guadecitabine allowed us only to hypothesize that the seven EV-miRNAs are more likely to be of stromal or immune origin (data not shown).

Investigating the origin of the EV-miRNAs with technologies that track EVs and simultaneously allow the evaluation of miRNA expression could shed light on their functional mechanism and potential involvement of these EV-miRNAs in tumor and immune microenvironment cells, underscoring their impact in shaping therapeutic responses and outcomes[20,21].

To reinforce the biological significance of the EV-miRNAs primary resistance signature, we re-analyzed transcriptional data from the same cohort of patients'[11]. We explored the enriched pathways of the DE genes in NR compared to R patients and evaluated whether they converged to the seven EV-miRNAs enriched pathways (Supplementary Data 8 and 9). Fourteen pathways were associated to cell cycle regulation among the top-enriched pathways in NR patients, supporting the link to pathways promoting tumor growth that we observed with the EV-downregulated miRNA-enriched pathways. Five apoptotic and nine metabolic pathways were among the bottom enriched pathways, lending support to the EV up-regulated miRNAs enriched pathways in NR that indicated activation of adaptive mechanisms that may contribute to tumor resistance.

Among the seven EV-miRNAs, the predictive value of four key EV-miRNAs (miR-497-5p, miR-99a-3p, miR-592, and miR-548b-3p) was validated in an independent cohort treated with ipilimumab monotherapy, achieving a remarkable predictive performance (AUC = 0.94) (Table 3).

The validation, which used serum samples from monotherapy-treated patients and employed ddPCR—a different technology from the discovery cohort—lends support on the use of these EV-miRNAs as biomarkers, as reflected in their higher performance.

All four EV-miRNAs have been previously described as being involved in melanoma[22–26]. MiR-497-5p, up-regulated in NR patients compared to R, is a highly conserved miRNA previously associated with immune evasion and anti-PD-1 resistance in hepatocellular carcinoma and colorectal cancer[27,28]. Its association with primary resistance to ICI in melanoma may

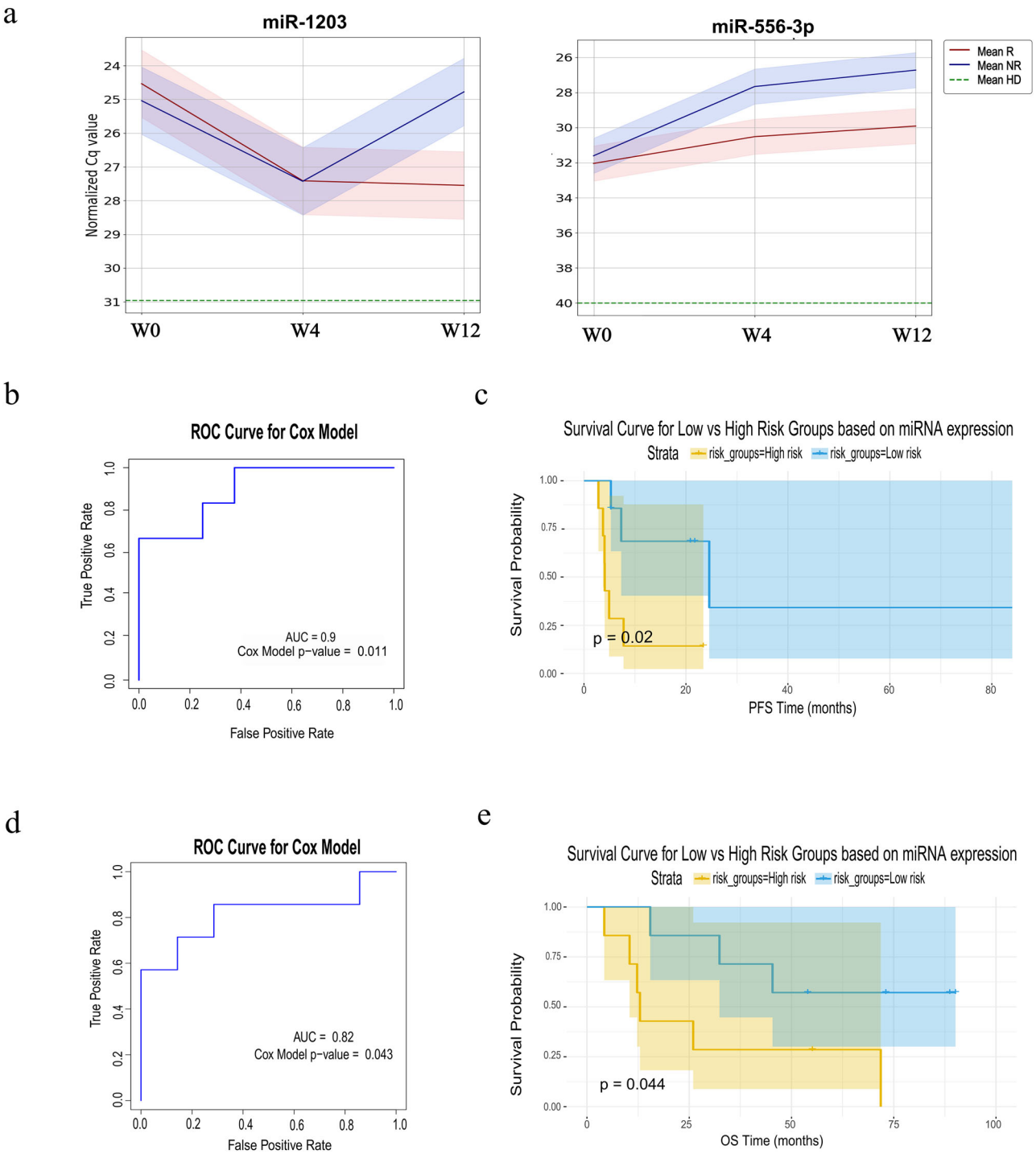

Fig. 6 | Predictive and monitoring roles of miR-1203 and miR-556-3p. **a** Expression of miR-1203 over time in NR and R. The plot displays the average normalized expression levels of miR-1203 (left panel) and miR-556-3p (right panel) at W0, W4, and W12 for patients classified as NR (blue) and R (red). Shaded areas represent the SEM. **b** ROC curve to assess the predictive accuracy of the combined COX model based on PFS, patient's status (alive or dead), miR-1203 and miR-556-3p expression for distinguishing patients with higher likelihood of survival in the NIBIT-M4 cohort at week 12. $P < 0.05$ were considered statistically significant. **c** Kaplan–Meier PFS curve of the combined Cox risk model; **d** ROC curve to assess the predictive accuracy of the combined Cox model based on OS, patient's status (alive or dead) and miR-1203 and miR-556-3p expression. **e** Kaplan–Meier OS curve of the combined Cox risk model based on OS and miR-1203 and miR-556-3p expression at week 12. W0 week 0 (baseline), W4 week 4, W12 week 12, PFS progression-free survival, OS overall survival, ROC receiver operating characteristic, SEM standard error of the mean.

involve dysregulation of apoptotic and metabolic pathways, as suggested by target enrichment analysis. MiR-99a-3p and miR-548b, down-regulated in NR compared to R, were strongly associated with pathways promoting tumor growth, including cell cycle regulation and Hippo signaling, suggesting a potential loss or attenuation of their tumor-suppressive roles. Notably, while previously linked to therapy resistance in non-ICI contexts across various tumor types, these miRNAs have also been implicated in the regulation of immune functions[29–32]. Further investigation of the validated target genes of the down-regulated EV-miRNAs (miR-497-5p, miR-99a-3p, miR-592, and miR-548b-3p) composing the primary resistance signature

Table 3 | EV-miRNAs signatures of therapy response

4 EV-miRNAs biomarkers of primary resistance	Expression levels NR vs. R (W0)
miR-497-5p	Up-regulated
miR-548-3p	Down-regulated
miR-99a-3p	Down-regulated
miR-592	Down-regulated
9 EV-miRNAs DE during treatment	**Expression levels W4 / W12 vs. W0**
miR-576-5p	Down-regulated
miR-150-3p	Down-regulated
miR-1183	Down-regulated
miR-604	Down-regulated
miR-892a	Down-regulated
miR-1203	Down-regulated
miR-26b-3p	Up-regulated
miR-34a-5p	Up-regulated
miR-556-3p	Up-regulated
2 EV-miRNAs biomarkers of secondary resistance and DE during treatment	**Expression levels NR vs. R (W12)**
miR-1203	Up-regulated
miR-556-3p	Up-regulated

Schematic summary of EV-miRNAs signatures associated with therapy response in metastatic melanoma patients treated with DHA + anti-CTLA4.

revealed six up-regulated genes in NR patients compared to R, also reported as highly expressed in other cancers and linked to therapy resistance (Supplementary Table 1).

Our findings suggest that the predictive utility of the primary resistance signature is associated to immunotherapy. Our data show that boosting immunotherapy with DHA does not have a direct impact in the primary resistance EV-miRNA signature.

In this study, we also identified 9 EV-miRNAs (miR-150-3p, miR-576-5p, miR-26b-3p, miR-34a-5p, miR-556-3p, miR-1183, miR-1203, miR-604, and miR-892a) that were consistently deregulated at both post-treatment time points, suggesting a therapy-modulated EV-miRNA signature (Table 3).

Among targets regulated by those EV-miRNAs, mitogen-activated protein kinase (MAPK), PI3K-AKT pathways are melanoma-specific and can influence the sensitivity to immunotherapeutic agents[33].

Moreover, among therapy modulated EV-miRNAs, miR-1203 and miR-507 were previously identified as part of diagnostic melanoma-specific EV-miRNAs signature[12], and are significantly down-regulated by week 12, suggesting their potential relevance in melanoma progression (Table 3).

Further analysis revealed that among therapy modulated EV-miRNA, only miR-1203 and miR-556-3p were significantly associated with the therapy response. These two miRNAs demonstrated strong predictive performance in ROC analysis and were significantly associated with survival (PFS and OS). Their early modulation underscores their value not only as prognostic biomarkers but also for relapse monitoring as early as four weeks post-treatment. Notably, both miR-1203 and miR-556-3p have been described in cancer progression[34–37], suggesting that their roles as biomarkers may extend beyond diagnostic applications to fundamental mechanisms underlying tumor development, aggressiveness, and therapy resistance. It is important to note that EV-miRNAs are not randomly distributed but selectively sorted into EVs to ensure their stable delivery to recipient cells, where they can modulate gene expression and mediate highly specific cell–cell communication[38]. For instance, miR-592 has been demonstrated to be preferentially incorporated into EVs derived from melanoma cancer stem cells, allowing it to influence target cell behavior[26].

Intercepting these EV-encoded messages, which often drive aggressive phenotypes, metastatic dissemination, or resistance to therapies, is of pivotal importance for understanding tumor biology. Indeed, EVs play a critical role in transmitting pro-survival, pro-metastatic, and therapy-resistant signals across the tumor microenvironment[38], including the transfer of RNA species that reprogram recipient cells toward a more malignant state[39].

Hence, identifying and targeting these selective EV-mediated communication pathways could open new therapeutic opportunities to intercept cancer progression and improve clinical outcomes.

While our findings align with this perspective, the intricate mechanisms at play remain to be fully elucidated. Emerging technologies, such as single-cell and spatial transcriptomics, are poised to provide valuable insights into the complex interplay between the tumor microenvironment, and immune system dynamics in the coming years[40–42].

The results of this study highlight how future research should focus on validating this EV-miRNA signature in larger, independent cohorts, as our findings are based on a relatively small and highly selected population of advanced melanoma patients treated within an exploratory guadecitabine plus ipilimumab trial. The predictive and monitoring value of the identified EV-miRNA signatures needs to be confirmed in larger, independent studies before they can be implemented in routine cancer patient management.

Further exploring the functional roles of these EV-miRNAs and their host genes within resistance mechanisms and immune modulation will be crucial. Unraveling their biological contributions to the tumor microenvironment could provide critical insights into resistance pathways, ultimately informing the development of novel therapeutic strategies and improving patient outcomes.

Data availability

The authors declare that all anonymized data supporting the findings of this study are available within the paper and its Supplementary Information files. EV-miRNA profiling data, source for Fig. 6a, b, d are available in Supplementary Data 1. Source data for Figs. 2 and 5 can be found in Supplementary Data 2. Source data for Fig. 3a, b can be found in Supplementary Data 3. Source data for Fig. 3c can be found in Supplementary Data 4. Source data for Fig. 4a, b can be found in Supplementary Data 5. Source data for Fig. 4c can be found in Supplementary Data 6. Source data for Fig. 6c–e can be found in Supplementary Data 7. Differentially expressed genes and enrichment pathway analysis of 8 NR compared to 6 R at baseline can be found in Supplementary Data 8 and 9.

Received: 19 August 2025; Accepted: 21 April 2026;
Published online: 08 May 2026

References

1. Svedman, F. C. et al. Extracellular microvesicle microRNAs as predictive biomarkers for targeted therapy in metastatic cutaneous malignant melanoma. *PLoS ONE* **13**, e0206942 (2018).
2. Kim, T. & Croce, C. M. MicroRNA: trends in clinical trials of cancer diagnosis and therapy strategies. *Exp. Mol. Med.* **55**, 1314–1321 (2023).
3. Metcalf, G. A. D. MicroRNAs: circulating biomarkers for the early detection of imperceptible cancers via biosensor and machine-learning advances. *Oncogene* **43**, 2135–2142 (2024).
4. Smith-Uffen, M., Park, J., Parsonson, A., Kiely, B. E. & Vasista, A. Estimating scenarios for survival time in patients with advanced melanoma receiving immunotherapy and targeted therapy. *Oncologist* **29**, 922–930 (2024).
5. Carlino, M. S., Larkin, J. & Long, G. V. Immune checkpoint inhibitors in melanoma. *Lancet* **398**, 1002–1014 (2021).
6. Van Allen, E. M. et al. Genomic correlates of response to CTLA-4 blockade in metastatic melanoma. *Science* **350**, 207–211 (2015).
7. Zhan, Y. et al. Extracellular vesicle-derived non-coding RNAs in remodeling melanoma. *Biomed. Pharmacother.* **172**, 116213 (2024).

8. Gahlawat, A. W., Witte, T., Sinn, P. & Schott, S. Circulating cf-miRNA as a more appropriate surrogate liquid biopsy marker than cfDNA for ovarian cancer. *Sci. Rep.* **13**, 5503 (2023).
9. Preethi, K. A. et al. Liquid biopsy: exosomal microRNAs as novel diagnostic and prognostic biomarkers in cancer. *Mol. Cancer* **21**, 54 (2022).
10. Di Giacomo, A. M. et al. Guadecitabine plus ipilimumab in unresectable melanoma: the NIBIT-M4 clinical trial. *Clin. Cancer Res.* **25**, 7351–7362 (2019).
11. Noviello, T. M. R. et al. Guadecitabine plus ipilimumab in unresectable melanoma: five-year follow-up and integrated multi-omic analysis in the phase 1b NIBIT-M4 trial. *Nat. Commun.* **14**, 5914 (2023).
12. Sabato, C. et al. A novel microRNA signature for the detection of melanoma by liquid biopsy. *J. Transl. Med.* **20**, 469 (2022).
13. identifying-mirna-normalizers-white-paper. https://www.thermofisher.com/content/dam/LifeTech/Documents/PDFs/miRNA-controls-WhitePaper.pdf
14. Tastsoglou, S. et al. DIANA-miRPath v4.0: expanding target-based miRNA functional analysis in cell-type and tissue contexts. *Nucleic Acids Res.* **51**, W154–W159 (2023).
15. Ma, L. et al. Liquid biopsy in cancer: current status, challenges and future prospects. *Signal Transduct. Target. Ther.* **9**, 1–36 (2024).
16. Splendiani, E. et al. Immunotherapy in melanoma: can we predict response to treatment with circulating biomarkers? *Pharmacol. Ther.* **256**, 108613 (2024).
17. Nobrega, M. et al. Comparative analysis of extracellular vesicles miRNAs (EV-miRNAs) and cell-free microRNAs (cf-miRNAs) reveals that EV-miRNAs are more promising as diagnostic and prognostic biomarkers for prostate cancer. *Gene* **939**, 149186 (2025).
18. Maio, M. et al. Molecular pathways: at the crossroads of cancer epigenetics and immunotherapy. *Clin. Cancer Res.* **21**, 4040–4047 (2015).
19. Covre, A. et al. Epigenetics meets immune checkpoints. *Semin. Oncol.* **42**, 506–513 (2015).
20. Hendriksen, J. D. et al. Immunotherapy drives mesenchymal tumor cell state shift and TME immune response in glioblastoma patients. *Neuro Oncol.* **26**, 1453–1466 (2024).
21. Adegoke, N. A. et al. Classification of the tumor immune microenvironment and associations with outcomes in patients with metastatic melanoma treated with immunotherapies. *J. Immunother. Cancer* **11**, e007144 (2023).
22. Feng, X.-E. miR-548b suppresses melanoma cell growth, migration, and invasion by negatively regulating its target gene HMGB1. *Cancer Biother. Radiopharm.* **36**, 189–201 (2021).
23. Chai, L. et al. MiR-497-5p, miR-195-5p and miR-455-3p function as tumor suppressors by targeting hTERT in melanoma A375 cells. *Cancer Manag. Res.* **10**, 989–1003 (2018).
24. Poell, J. B. et al. A functional screen identifies specific MicroRNAs capable of inhibiting human melanoma cell viability. *PLoS ONE* **7**, e43569 (2012).
25. Bagheri, M. S. et al. Preoperative plasma miRNA levels predict prognosis in early-stage malignant melanoma. *Anticancer Res.* **43**, 695–706 (2023).
26. Zhang, Y. et al. Extracellular vesicles microRNA-592 of melanoma stem cells promotes metastasis through activation of MAPK/ERK signaling pathway by targeting PTPN7 in non-stemness melanoma cells. *Cell Death Discov.* **8**, 428 (2022).
27. Ye, R. et al. CircSOD2 contributes to tumor progression, immune evasion and anti-PD-1 resistance in hepatocellular carcinoma by targeting miR-497-5p/ANXA11 axis. *Biochem. Genet.* **61**, 597–614 (2023).
28. Xu, Y.-J. et al. Hsa_circ_0136666 activates Treg-mediated immune escape of colorectal cancer via miR-497/PD-L1 pathway. *Cell Signal.* **86**, 110095 (2021).
29. Tian, X., Liu, J., Yi, C., You, X. & Yuan, C. Hsa_circ_0072732 enhances sunitinib resistance of renal cell carcinoma by inhibiting ferroptosis. *Discov. Oncol.* **15**, 700 (2024).
30. Angerilli, V. et al. MicroRNAs as predictive biomarkers of resistance to targeted therapies in gastrointestinal tumors. *Biomedicines* **9**, 318 (2021).
31. Hua, M. et al. Aberrant expression of microRNA in $CD4^+$ cells contributes to Th17/Treg imbalance in primary immune thrombocytopenia. *Thromb. Res.* **177**, 70–78 (2019).
32. Souza, M. deA. et al. miR-548d-3p alters parasite growth and inflammation in *Leishmania* (*Viannia*) *braziliensis* infection. *Front. Cell Infect. Microbiol.* **11**, 687647 (2021).
33. Alsaafeen, B. H., Ali, B. R. & Elkord, E. Resistance mechanisms to immune checkpoint inhibitors: updated insights. *Mol. Cancer* **24**, 20 (2025).
34. Shi, J. et al. MiR-1203 is involved in hepatocellular carcinoma metastases and indicates a poor prognosis. *Neoplasma* **67**, 267–276 (2020).
35. Al-Asadi, S., Mansour, H., Ataimish, A. J., Al-Kahachi, R. & Rampurawala, J. MicroRNAs regulate tumorigenesis by downregulating SOCS3 expression: an in silico approach. *Bioinform. Biol. Insights* **17**, 11779322231193535 (2023).
36. Zhou, Y. et al. QKI-induced circ_0001766 inhibits colorectal cancer progression and rapamycin resistance by miR-1203/PPP1R3C/mTOR/Myc axis. *Cell Death Discov.* **11**, 192 (2025).
37. Hao, Q. et al. Hsa_circRNA_001676 accelerates the proliferation, migration and stemness in colorectal cancer through regulating miR-556-3p/G3BP2 axis. *Sci. Rep.* **13**, 18353 (2023).
38. Garcia-Martin, R. et al. MicroRNA sequence codes for small extracellular vesicle release and cellular retention. *Nature* **601**, 446–451 (2022).
39. Parashar, D., Mukherjee, T., Gupta, S., Kumar, U. & Das, K. MicroRNAs in extracellular vesicles: a potential role in cancer progression. *Cell Signal.* **121**, 111263 (2024).
40. Robert, C. & Gautheret, D. Multi-omics prediction in melanoma immunotherapy: a new brick in the wall. *Cancer Cell* **40**, 14–16 (2022).
41. Hunter, M. V., Moncada, R., Weiss, J. M., Yanai, I. & White, R. M. Spatially resolved transcriptomics reveals the architecture of the tumor-microenvironment interface. *Nat. Commun.* **12**, 6278 (2021).
42. Love, N. R. et al. Melanoma progression and prognostic models drawn from single-cell, spatial maps of benign and malignant tumors. *Sci. Adv.* **10**, eadm8206 (2024).

Acknowledgements

The authors would like to acknowledge all the support staff at the participating institutions for their contributions to this study, the patients who participated in this study and their families. This research was supported by co-funding of the European Union – The National Recovery Plan, mission 4 component 2 investment 1.4 – Next Generation EU project CN3-Spoke 2 Cancer-code CN_00000041 (CUP: B83C22002870006), Associazione Italiana per la Ricerca sul Cancro (AIRC) Project "5 per Mille" EPICA [grant number 21073] and Ministero della Salute, Regione Toscana e Regione Lombardia [grant number NET-2016-02361632, P.I. Michele Maio].

Author contributions

Conceptualization: A.C., S.C., A.P., M.M., A.M.D.G., and E.F. Data curation: E.S., Z.M.B., C.S., and T.M.R.N. Formal analysis: E.S., Z.M.B., C.S., T.M.R.N., F.P.C., A. Citarella, G.C., A.M.D.G., and M.C. Funding acquisition: M.M., M.C., and E.F. Investigation: E.S., C.S., Z.M.B., T.M.R.N., M.F.L., V.D'A., M.V., L.S., I.S., A.C., A.P., A. Citarella, G.C., M.M., M.C., and E.F. Methodology: E.S., C.S., Z.M.B., T.M.R.N., F.P.C., T.M.A., R.M., and A.A. Project administration: A.C., S.C., M.M., E.F., and A.M.D.G. Resources: M.M., M.C., and E.F. Supervision: M.M., M.C., A.M.D.G., and E.F. Validation: E.S., T.M.A. Writing-original draft: E.S., Z.M.B., A.P., and E.F. Writing review

and editing: All. Final approval: All authors have read and approved of the final manuscript.

Competing interests
The authors declare no competing interests.

Additional information
Supplementary information The online version contains Supplementary material available at https://doi.org/10.1038/s43856-026-01629-z.

Correspondence and requests for materials should be addressed to Anna Maria Di Giacomo or Elisabetta Ferretti.

Peer review information *Communications Medicine* thanks Christoforos Vaxevanis, Xiaochao Tan and the other anonymous reviewer(s) for their contribution to the peer review of this work. A peer review file is available.